Ultrafast carrier relaxation in GaN, $In_{0.05}Ga_{0.95}N$ and an $In_{0.05}Ga_{0.95}N/In_{0.15}Ga_{0.85}N$ Multiple Quantum Well

Ümit Özgür, and Henry O. Everitt[*]

Department of Physics, Duke University, Durham, NC 27708

(Dated: February 1, 2008)

Room temperature, wavelength non-degenerate ultrafast pump/probe measurements were performed on GaN and InGaN epilayers and an InGaN multiple quantum well structure. Carrier relaxation dynamics were investigated as a function of excitation wavelength and intensity. Spectrally-resolved sub-picosecond relaxation due to carrier redistribution and QW capture was found to depend sensitively on the wavelength of pump excitation. Moreover, for pump intensities above a threshold of 100 $\mu J/cm^2$, all samples demonstrated an additional emission feature arising from stimulated emission (SE). SE is evidenced as accelerated relaxation (< 10 ps) in the pump-probe data, fundamentally altering the re-distribution of carriers. Once SE and carrier redistribution is completed, a slower relaxation of up to 1 ns for GaN and InGaN epilayers, and 660 ps for the MQW sample, indicates carrier recombination through spontaneous emission.

I. INTRODUCTION

Technological advances in group-III nitride-based optoelectronics have been possible with extensive materials research, resulting in the commercialization of short wavelength emitters and detectors.[1,2,3,4] The active layers in high efficiency emitters, such as blue/green light emitting diodes and blue/purple laser diodes, contain InGaN alloys. Time scales for carrier recombination, transport, and quantum well capture in the ultrafast regime determine the efficiency of optoelectronic devices. Therefore it is important to understand the carrier relaxation and recombination mechanisms in InGaN structures. In addition to many studies on recombination times,[5,6,7] there have been a limited number of reports on ultrafast carrier dynamics in InGaN heterostructures[8,9] and multiple quantum wells (MQW).[10,11] Measurements on heterostructures, single QWs, and MQWs have emphasized different aspects of carrier relaxation in nitrides. In this paper, we report comprehensive room temperature ultrafast measurements on a bulk GaN, an InGaN epilayer, and an InGaN MQW sample having barriers with the same In composition as the epilayer sample.

In achieving the current state of nitride device development, overcoming material growth difficulties has been the main focus. The efficiencies of InGaN-based emitters are strongly affected by material inhomogeneities such as compositional fluctuations and indium-phase separation. However, inhomogeneities in the form of quantum dot-sized In-rich regions are observed to increase lateral confinement, thereby increasing the emission efficiencies of InGaN devices. The effect of these In-rich regions on electron-hole recombination through spontaneous emission (SPE) has been studied extensively.[5,12,13] In spite of imperfect material properties, high emission efficiencies are observed not only through enhanced SPE but also through stimulated emission (SE) generated at moderate pump powers. There have been many reports on SE in InGaN epilayers[14,15] and MQW structures.[16,17,18] However SE and its effects on carrier relaxation is poorly under-stood. In this study, ultrafast dynamics in the presence and absence of SE are investigated.

Three samples, a GaN epilayer, an InGaN epilayer, and an InGaN MQW structure, were grown on c-plane double polished sapphire by metalorganic chemical vapor deposition at the University of California, Santa Barbara.[19] The GaN sample is ~ 3 μm thick, and the buffer layers in the other two samples are ~ 2 μm thick GaN:Si. InGaN epilayer sample consists of a 60 nm thick $In_{0.05}Ga_{0.95}N$:Si layer, capped with another 15 nm thick GaN layer. The InGaN MQW is a typical laser active layer structure with 10 periods of 8.5 nm $In_{0.05}Ga_{0.95}N$:Si barriers and 3.5 nm $In_{0.15}Ga_{0.85}N$ quantum wells. There is a 100 nm GaN cap layer on top of the MQW. The doping in the barriers and in the InGaN epilayer is $\sim 10^{18}$ cm^{-3}.

In section II, techniques used in the experiment are introduced. Then the results for each sample are respectively considered as subsections of section III. In each subsection, first continuous-wave (cw) and time integrated measurements are presented to identify the band structures. The investigation of carrier relaxation dynamics follows, using non-degenerate time-resolved differential transmission (TRDT) spectroscopy. To understand the effects of the underlying buffer and cap GaN layers, and to understand the effects of the 3D InGaN barriers in the MQW sample, measurements on the bulk GaN sample and on the InGaN epilayer sample are discussed, respectively. Above- and below-bandgap excitation data are presented to explore the excitation wavelength dependence of the GaN and InGaN relaxation phenomena.

Similarly, measurements on the MQW sample are reported for above-, at-, and below-barrier energy excitations. Time-resolved data for the MQW sample are compared with results from a previous study of carrier capture times using degenerate TRDT.[20]

II.   EXPERIMENTAL TECHNIQUES

A.   Continuous wave and time-integrated characterization

Continuous-wave (cw) photoluminescence (PL), PL excitation (PLE), and absorption measurements were performed at room temperature. Cw-PL was measured at excitation power densities of 100 W/cm^2 using a 25 mW HeCd laser operating at 325 nm (3.82 eV). A 300 W Xe Lamp was used for PLE and cw-absorption measurements. Xe Lamp was dispersed by a 30 cm double grating spectrometer for the PLE, and both cw-PL and PLE were detected by a photomultiplier tube attached to a 75 cm grating spectrometer. Another 30 cm grating spectrometer with a charge coupled device (CCD) was used for the absorption measurements.

Pulsed excitation, time-integrated PL (TI-PL) is performed on the samples at room temperature using 1 kHz, ∼10 μJ pulses from an optical parametric amplifier, at excitation power densities varied between 20 μJ/cm^2 and 2 mJ/cm^2, either by changing the focus or using neutral density filters. For high enough excitation densities, SE features are observed for all the samples. To obtain the SE threshold densities, PL from the samples was detected both normal to the surface from the front and parallel to the surface from the edges. Edge detection produced stronger SE signals, making it the preferred detection scheme. The samples were excited normal to the surface, and the PL was collected from the edge using a 600 μm diameter UV-VIS fiber. A CCD attached to the 30 cm spectrometer was used for detection. Both the spectrally-integrated PL intensity and the emission linewidth were plotted as a function of pump power density and found to give identical SE thresholds.

B.   Time-resolved characterization

Previously, standard wavelength-degenerate, time-resolved differential transmission (TRDT) measurements were performed on the MQW sample, using a frequency-doubled mode-locked Ti:Sapphire laser.[20] In this study, non-degenerate TRDT spectroscopy was applied at room temperature. A Ti:Sapphire laser-seeded, 1 kHz Quantronix Titan regenerative amplifier (RGA) with 1.8 mJ , 100 fs pulses at 800 nm was used. Half of the RGA output power is used to pump a Quantronix TOPAS optical parametric amplifier (OPA). The signal output from the tunable OPA is frequency quadrupled and used as the pump in the DT experiment. The other half of the RGA output is frequency doubled in a BBO crystal and focused on a quartz cell filled with D_2O to generate a broadband continuum probe centered near 400 nm (3.11 eV). The continuum probe, which has relatively minor amplitude fluctuations over its > 100 nm bandwidth, is highly attenuated by spatial filtering, then collected and focused on the sample using a spherical mirror. The pump beam

is delayed with respect to the probe beam using a retroreflector mounted on a 1 μm-resolution translational stage. The probe, transmitted through the sample, is then collected by a UV liquid light guide, sent to the 30 cm grating spectrometer, and detected by a CCD camera attached to the output port. It is important to note that the excitation regime in this study is much higher (>100 μJ/cm^2) than the previous study of degenerate TRDT (∼1 μJ/cm^2).[20] Using a pump intensity-independent absorption constant of 10^5 cm^{-1},[21] the number of photo-injected carriers in the MQW sample is estimated to be 10^{17} cm^{-3} for the previous study, and >10^{19} cm^{-3} for this work. These carrier densities are larger for the GaN sample due to its larger thickness.

First, the continuum probe spectrum is recorded. Next, the pulsed absorption spectrum of the sample is obtained by comparing the continuum probe spectrum and the spectrum of the probe transmitted through the unpumped sample. Some absorption features that were not clear in the cw-absorption data were easily observed in the pulsed absorption spectra due to larger excitation density. Then, pump-probe measurements are made by comparing the transmission of the probe through the sample with and without the pump beam for various delays up to 0.4 ns. The absolute DT signal at energy hν is

$$DT(h\nu) = \frac{T_{PumpON}(h\nu) - T_{PumpOFF}(h\nu)}{T_{PumpOFF}(h\nu)} = -\triangle\alpha(h\nu)d, \tag{1}$$

where T_{PumpON} and $T_{PumpOFF}$ are the probe transmission signal magnitudes with the pump beam on and off, respectively. $\triangle\alpha$ is the change in the absorption coefficient, and d is the thickness of the sample over which the change in absorption is induced. Pump and probe spot diameters on the samples were ∼1 mm and ∼0.2 mm, respectively. The absorption from the bare probe beam was observed to be much smaller than the absorption due to the pump beam, suggesting that the modulation in the DT signal is purely from the pump.

TRDT data is presented in two different ways, spectrally-integrated and spectrally-resolved, in order to elucidate different aspects of the relaxation processes. Spectrally-integrated DT gives an indication of the total population of carriers (i.e. density of states) and their aggregate decay, while spectrally-resolved DT describes the distribution of carriers and indicates their energy relaxation pathways.

Due to the thick GaN layers, strong absorption at the GaN band edge allows only weak transmission of the probe beam for all the samples. Therefore, a small pump-induced change in the absorption at the GaN energy will yield a large TRDT signal. Spectrally-resolved TRDT data for all the samples show oscillations that arise from the interference of the multiple reflections in the sample.

Similar non-degenerate TRDT measurements have been performed on GaN,[22,23] InGaN epilayers[8,9], and In-GaN MQWs[9,10,11,24], by different groups. These studies provide insights on important aspects of carrier relax-
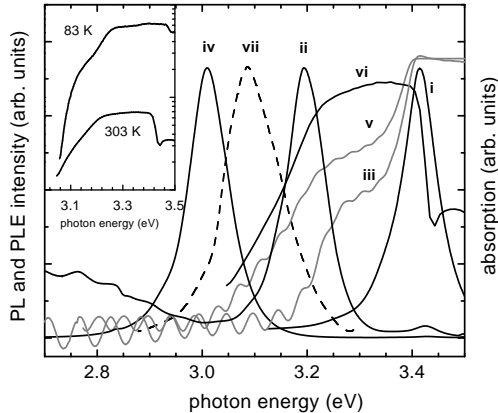
FIG. 1: Room temperature cw-PL(i) for the GaN sample, cw-PL(ii) and absorption(iii) for the InGaN sample, cw-PL(iv), cw absorption (v), PLE (vi) and time integrated pulsed-PL (vii) for the MQW sample. The excitation density for the pulsed-PL is above ($\sim$2 mJ/cm^2) the SE threshold. Inset shows the log scale plot of the 83 K and 303 K PLE for the MQW sample.

ation dynamics. In this study, a more comprehensive investigation is made, focusing on relaxation over many time scales, sub-picosecond to nanosecond, as a function of excitation wavelength and density. The role of stimulated emission on carrier dynamics is also studied in both spectrally-integrated and spectrally-resolved data.

III.   RESULTS AND DISCUSSION

A.   Differential transmission of bulk GaN

The cw-PL from the bulk GaN sample is centered at 3.41 eV (Fig. 1) when excited above (3.82 eV) the bandgap, in agreement with the 3.41 eV GaN band edge obtained from pulsed absorption measurements. Pulsed-PL showed another peak at 3.31 eV due to electron-hole plasma (EHP) induced SE[25,26,27] with a threshold of 70 μJ/cm^2. The SE peak is observed to redshift by 25 meV and broaden (from 37 meV to 66 meV) with increasing pump intensity (from 40μJ/cm^2 to 2 mJ/cm^2). When the sample is excited below (3.34 eV) the bandgap, no PL is observed.

The spectrally-integrated TRDT data for the GaN at excitation energies above (3.82 eV) and below (3.34 eV) the bandgap are shown in Fig. 2. For below bandgap excitation, increased transmission is observed for a very short time, less than 1 ps. Data for the above bandgap excitation shows a similarly rapid rise ($<$ 1 ps), a $\sim$2 ps-wide peak, and a fast decay (3-6 ps), followed by a much slower relaxation (100's of ps). For both excitations, the early, strong increase in transmission at the GaN band edge is due to photo-excited carriers and the
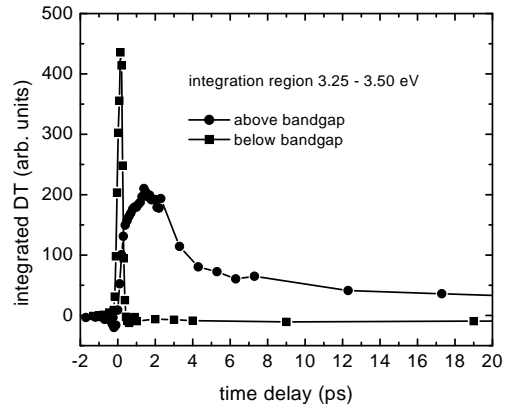

FIG. 2: Time evolution of the spectrally-integrated TRDT for above (circles) and below (squares) bandgap excitations of the bulk GaN sample at an excitation power density of 300 μJ/cm^2. Integration region was 3.25 eV - 3.50 eV.

dynamic (AC) Stark effect.[22,28] The wide peak and fast relaxation are due to the operation and removal of carriers through SE, which occurs when the pump density is above threshold (70 μJ/cm^2) and ends when the number of carriers is reduced below threshold. The time constant for SE decay at excitation density of 300 μJ/cm^2 is measured to be $\sim$2 ps.

Spectrally-resolved results from the TRDT measurements on the GaN sample (Fig. 3) confirm these findings for excitations above and below the GaN band edge. For above bandgap excitation (Fig. 3a), the carrier distribution is broad ($\sim$80 meV) and extends below the bandgap ($\sim$3.34 eV) during the first 1.2 ps. The carriers relax to the GaN band edge in $\sim$ 2ps through multiple LO-phonon and carrier scattering events required to cool the carriers as much as 400 meV.[29] The 2 ps-wide SE feature in the spectrally-integrated DT is observed during this cooling. After 2 ps when the carrier redistribution is finished, a clear decay due to SE becomes visible, with a decay constant of $\sim$ 2 ps. At later times (17 ps), the lower energy part (3.34 eV - 3.37 eV) of the distribution disappears, while carriers near the GaN band edge show increasing absorption. The decay of the low energy part might be explained by the blueshift of the SE, and carrier energy, in the EHP after the number of carriers is decreased through SE. This is supported by the fact that SE redshifts with increasing carrier density due to increased coulombic repulsion.[26]

For excitation 80 meV below the bandgap (Fig. 3b), the generation of carriers may seem more surprising, especially because it cannot be explained as an assist from room temperature thermal energy k$_B$T (26 meV) or from the pulse bandwidth (25 meV). It is well known that the excitonic resonances are visible even at room temperature for GaN[21], and AC Stark effect has been observed for GaN for detunings as large as 159 meV below the exci-
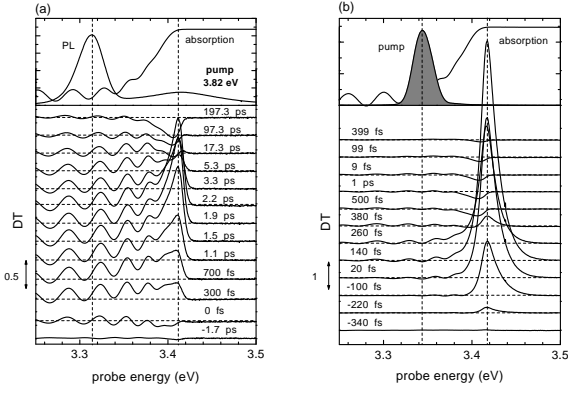
FIG. 3: Spectrally-resolved TRDT for above (a) and below (b) bandgap excitations of the bulk GaN sample at various delays for an excitation density of 300 μJ/cm^2. The top graphs show the pump spectrum, the TI-PL, and the pulsed absorption.
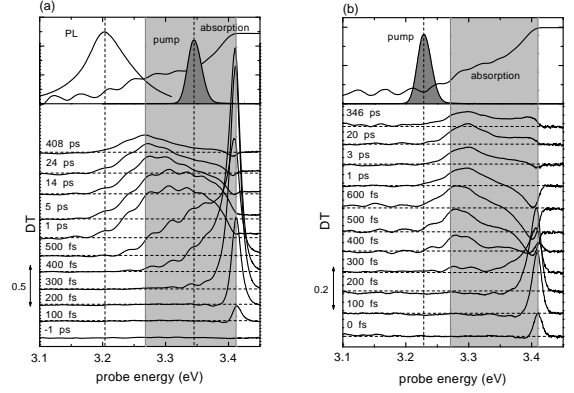

FIG. 4: Spectrally-resolved TRDT for above (a) and below (b) bandgap excitations of the InGaN epilayer sample at various delays for an excitation density of 300 μJ/cm^2. The top graphs show the pump spectrum, the TI-PL, and the pulsed absorption. The shaded regions indicate the states between GaN and InGaN band edges.

tonic resonance.[28] The bleaching which exists during the intense pump pulse and lasts less than 500 fs is an indication of the AC Stark effect. This short-lived AC Stark feature in Fig. 3b is observed in all the samples as the very fast increase and decay of the spectrally-integrated DT for below band gap excitations (e.g. Fig. 2). The residual change in the DT which persists as long as 400 ps is due to real excitation of carriers by the two-photon absorption of the intense pump pulse (300 μJ/cm^2).

At longer delays, induced absorption is observed at the GaN energy for both above and below band gap excitations. The observed slow relaxation is due to decaying remnant carriers and excitons at the GaN band edge. The rate of this decay is observed to be slower than 300 ps, which is consistent with the recombination lifetimes obtained for GaN.[21,27]

B. Differential transmission of an In$_{0.05}$Ga$_{0.95}$N epilayer

The PL emission from the In$_{0.05}$Ga$_{0.95}$N epilayer (Fig. 1) occurred at $\sim$3.20 eV for cw excitation (100W/cm^2) from the HeCd laser (3.82 eV). This is slightly lower than the band gap values for In$_{0.05}$Ga$_{0.95}$N in the literature, constrained between 3.220 eV to 3.224 eV.[30,31] TI-PL is only observed for above bandgap excitation, never for below bandgap excitation. The cw-absorption (Fig. 1) suggests an In$_{0.05}$Ga$_{0.95}$N band edge of 3.26 eV. When the broadening of the band edge is taken into account, an effective band edge of 3.22 eV is obtained from a sigmoidal fit[12], giving a 20 meV Stokes' shift. Since the piezoelectric (PZE) field in the InGaN epilayer is already reduced remarkably with Si doping, the band edge changes very little with pulsed laser excitation. Thus, screening of the PZE field does not produce a remarkable blueshift. This is verified by pulsed absorption measurements which suggest an In$_{0.05}$Ga$_{0.95}$N band
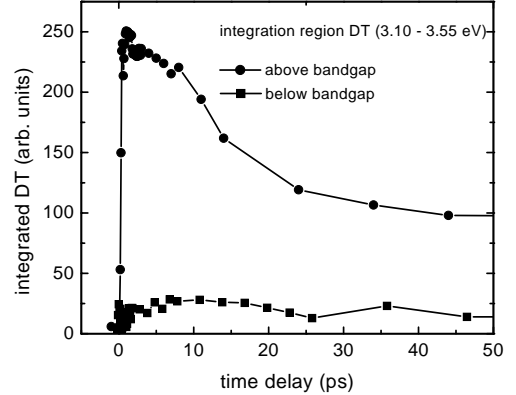
FIG. 5: Time-evolution of the spectrally-integrated TRDT for above (circles) and below(squares) bandgap excitations of the InGaN epilayer sample at an excitation density of 300 μJ/cm^2. Integration region was 3.10 eV - 3.55 eV.

edge of $\sim$3.26 eV, similar to the cw-absorption.

The spectrally-resolved TRDT data for the InGaN sample is shown in Fig. 4. Pump wavelengths for Fig. 4a and Fig. 4b were above (3.35 eV) and just below (3.23 eV) the InGaN bandgap, respectively. Before considering carrier dynamics in the InGaN layer, it is useful to reconsider carrier dynamics in the GaN layers in this sample. The pump energies are 60 meV, and 180 meV below the GaN bandgap, respectively. As in the below bandgap data for bulk GaN (Fig. 3b), it is first observed that the transmission increases from carrier generation and AC Stark effect in the GaN, reaching a maximum in $\sim$ 300 fs at the GaN band edge (3.41 eV) for both pump energies. AC Stark effect is observed in the GaN layers of the InGaN epilayer sample in a manner similar to the below band gap excitation of the GaN sample. The magnitude

of the AC Stark effect is smaller for the larger detuning of 190 meV in Fig. 4b. Real carriers are also generated at the GaN band edge due to two-photon absorption, but unlike the GaN sample they can quickly (<1 ps) decay into lower InGaN states through carrier-LO phonon and carrier-carrier scattering processes. This makes the distinction between the two-photon absorption and the AC-Stark effect more difficult. The small decreases (above bandgap) or increases (below bandgap) in absorption at the GaN band edge (3.41 eV) after 5 ps are due to the remnant carriers and excitons at the GaN interface and trap states. The two-photon induced carrier absorption feature in bulk GaN (Fig. 3b) remains visible after 408 ps with no remarkable reduction in its amplitude. This contrasts with the more complex induced absorption and transmission in the GaN cap and buffer layers of the In-GaN sample (Fig. 4b) which varies with excitation energy and time but remains for at least 400 ps. The differences can be attributed to carrier relaxation from the GaN layers to the InGaN epilayer and the reduced role of SPE in the GaN layers and trap states.

Regarding carrier dynamics in the InGaN layer, SE appears at 3.21 eV, near the InGaN band edge and slightly on the blue side (10 meV) of the PL, for excitation above (3.35 eV) the InGaN bandgap. Since the SE peak is broad and very close to the main PL peak, the onset of SE is observed as the emergence of a narrower linewidth PL whose strength increases with increasing pump intensity. From PL measurements of spectrally-integrated intensity and linewidth, a pump threshold of $\sim$80 μJ/cm^2 is obtained. Spectrally-integrated TRDT data for above bandgap, above threshold (300 μJ/cm^2) excitation shows a fast decay during the first 14 ps due to carrier removal through SE, followed by a much slower relaxation through SPE after the carrier density decreases below the SE threshold (Fig. 5). The fast rising edge of the spectrally-integrated dt for both excitations include the contribution from the AC Stark effect at the GaN band edge, as observed in Fig.2.

The fast relaxation feature of the spectrally-integrated TRDT is spectrally-resolved in Fig. 4a as a redistribution of the carriers. The broad distribution of carriers becomes clearly visible after 400 fs as a bleaching of the InGaN photo-absorption. The carrier distribution extends from the GaN band edge to the InGaN band edge and reaches a maximum in 1 ps at $\sim$ 3.30 eV. Afterwards, the blue edge of this bleaching, $\sim$ 70 meV above the InGaN band edge, is observed to decay rapidly (< 14 ps) while the red edge (3.18-3.27 eV) remains almost constant. The red shift of the bleaching arises from carrier cooling, and the peak reaches the In$_{0.05}$Ga$_{0.95}$N band edge (3.26 eV) by 14 ps when SE ceases. Thus the fast decay feature of the spectrally-integrated TRDT is due to the fast removal of the carriers at the InGaN band edge through SE, while carriers at higher energies relax down to refill the lost carriers. After the number of carriers is reduced below the SE threshold, only SPE remains.

By contrast, for the below bandgap excitation (3.23 eV), SE is not observed, and the DT signal, shown in Fig. 4b, does not exhibit SE-related features. The number of induced carriers is smaller, and the DT signal shows them narrowly distributed close (3.27 eV) to the band edge, reaching a maximum in 600 fs. Of particular noteworthiness is the absence of the SE-mediated fast decaying blue edge seen in above bandgap excitation. During the first 3 ps, there is also a more complex absorption change at the GaN band edge due to a combined effect of the AC Stark effect and the two-photon absorption. Induced absorption is observed after 400 fs until 3 ps, and increased transmission at the GaN energy persists for as long as 346 ps due to carriers and excitons in GaN trap states.

Spectrally-integrated DT data for both excitations show an additional decay component in the InGaN with a much larger time constant of several 100 ps. Spectrally-resolved TRDT reveals that carriers decay very slowly, and the carrier distribution continues to narrow, after 24 ps in above bandgap excitation (Fig. 4a) and after 600 fs in below bandgap excitation (Fig. 4b). The slow decay of these cooled carriers is due to radiative recombination-induced SPE. From the data, the radiative recombination time in this InGaN layer is estimated to be 0.98±0.08 ns, a value consistent with the reports in the literature.[5,32] Other TRDT measurements on InGaN epilayers[8,9] show similar slow decay behavior as in In$_{0.05}$Ga$_{0.95}$N epilayer investigated here.

C. Differential transmission of an InGaN MQW

1. Investigation of Sample Structure

As seen in Fig. 1, the cw-PL for the MQW sample shows a single emission centered at $\sim$3.01 eV associated with the confined QW minimum. The corresponding PLE and cw-absorption measurements indicate the In$_{0.05}$Ga$_{0.95}$N barrier energy is $\sim$3.23 eV. This barrier energy is 30 meV below the band edge energy obtained for the In$_{0.05}$Ga$_{0.95}$N epilayer because the barrier composition is slightly different, most probably due to In incorporation into the barriers from the wells.

Simple 1-D calculations predict the minimum confined QW energy level within 60 meV of the measured 3.01 eV, given reasonable values for conduction:valence band offsets (20:80 TO 80:20) and bowing parameter (1.75 eV)[30]. The difference between the measured and calculated values is satisfactory given the large but uncertain PZE field strength arising from lattice mismatch-induced strain between the layers.[33]

PLE at room temperature (Fig. 1) shows clear edges at the GaN and the In$_{0.05}$Ga$_{0.95}$N barrier energies consistent with the cw-absorption. The contribution from the confined QW states is not observed in cw-absorption. However, the logarithmic plot of the PLE signals at 303 K and 83 K (Fig. 1 inset) shows the broad QW edge at $\sim$3.11 eV and $\sim$3.14 eV, respectively. At tempera-

ture the emission is 100 meV lower than this PLE edge, but a sigmoidal fit to this QW edge gives an effective band edge of 3.06 eV, and a Stokes' shift of 50 meV. Shifts even larger than 300 meV have been observed for higher In composition MQWs under cw excitation.[7,12]

High excitation density TI-PL from the MQW sample produced a blueshift as large as 90 meV from the low intensity cw-PL peak. Similar to the SE feature of the InGaN epilayer, the MQW SE emission peak is not observed as a narrow feature on the main PL. Instead, just above the threshold ($\sim$95 μJ/cm^2), the emission peak narrows and blueshifts 20 meV. As excitation intensity increases, this narrowed emission continues to blueshift. This blueshift is primarily due to increased screening of the PZE field and to lateral carrier confinement in the MQW. As in the InGaN epilayer, the strain-induced PZE field of the MQW is decreased through Si doping and through screening by the large number of carriers induced by the pulsed laser.[7] MQW lateral carrier confinement arises from the formation of In-rich quantum dot-like regions in the QWs which grow with increasing In composition.[5] Such inhomogeneities have been observed for InGaN MQWs having even less than 15 % In.[7,35] Carrier localization due to inhomogeneities is also expected to decrease with Si doping in the barriers.[34] As the size of In-rich regions grow, the confinement within large dots is reduced and the Stokes' shift increases. The degree of confinement added to the screening of the PZE field make the blueshift in the MQW TI-PL larger than it is for the InGaN epilayer sample.

2. Spectrally-integrated and -resolved TRDT

To examine the relaxation of the total number of carriers, DT signals are integrated over the spectrum 2.92 - 3.41 eV for excitation energies above (3.35 eV), at (3.23 eV), and below (3.14 eV) the barrier energy.[36] As seen in Fig. 7, all three spectrally-integrated TRDT signals show a fast decay at early times, followed by a very slow relaxation. The fast components are observed to decay in less than 10 ps. Spectrally-integrated DT data were fit by a bi-exponential decay function, $Ae^{-t/\tau_1} + Be^{-t/\tau_2}$, where τ_1 and τ_2 are the decay times for the fast and the slow decaying components, and A and B are the corresponding amplitudes. A fractional strength value ($f = A/(A+B)$) is defined to observe the relative strength of the fast decaying component.

The fractional strength (f) of the fast decaying component is largest for at-barrier excitation, and is larger for above-barrier excitation than for below-barrier excitation (Inset, Fig. 7). As with the GaN and InGaN epilayers, the fast decay in the MQW sample is caused by the accelerated relaxation of carriers through SE. However, SE is observed even for below-barrier excitation of the MQW sample. For at-barrier energy excitation (SE threshold $\sim$ 95 μJ/cm^2), the magnitude of the fast feature is observed to decrease (f=0.74, 0.65 , 0.26) and its decay constant
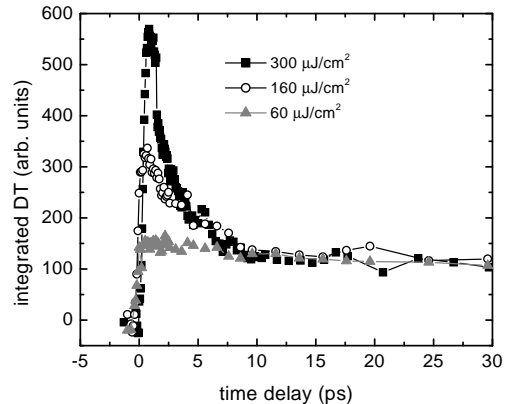

FIG. 6: Time-evolution of the spectrally-integrated TRDT for at-barrier excitation of the InGaN MQW sample for different pump power densities. Data were normalized to the slow decaying amplitude. With decreasing power density the SE-mediated fast decaying component is observed to disappear.
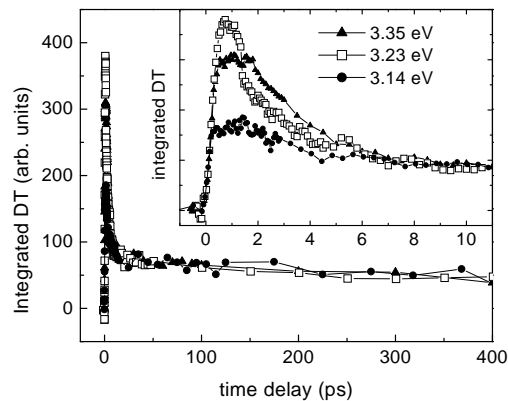

FIG. 7: Time-evolution of the spectrally-integrated TRDT for above- (triangles), at- (squares) and below-barrier (circles) bandgap excitations of the InGaN MQW sample at an excitation density of 300 μJ/cm^2. Integration region was 2.95 eV - 3.40 eV. Inset shows the fast decay components of the data.

slowed (2.6, 4.6, and 13.5 ps) as the excitation density decreased (300, 160, and 60 μJ/cm^2)(Fig. 6).[37] For a given excitation density (300 μJ/cm^2), the fast feature decay times for at-, above-, and below- barrier excitations increased (2.6, 2.6, and 3.7 ps, respectively)(Fig. 7), and the magnitude of the feature decreased (f=0.74, 0.73, 0.56), in a manner consistent with the strength of the PLE measured at the respective excitation energies (Fig. 1).

SE decay times faster than 10 ps have been observed for similar MQW structures at room temperature and at 2 K.[11,24] In one study, a three-level rate equation model was also developed, consisting of 2D QW, 3D barrier,

and ground (recombined) states.[11] This model suggested that the fast relaxation was due to carriers decaying from the 3D states to refill the 2D states emptied by SE. The fact that higher energy 3D states supply carriers to lower energy states undergoing SE has been confirmed in the GaN (Fig. 3a) and InGaN (Fig. 4a) data presented above. As will be discussed below, a similar process occurs in the MQWs, in which 3D states supply carriers for the saturated 2D states undergoing SE. Thus, SE reduces the total number of carriers in a similar manner for all samples studied.

To elucidate the carrier redistribution and relaxation processes, spectrally-resolved TRDT data for the InGaN MQW sample for various delays at different pump energies above, at, and below the barrier energy are shown in Fig. 8. The fast decaying AC-Stark and the two-photon absorption feature at the GaN energy (3.41 eV) is observed at all pump excitation energies and behaves analogously to the below GaN bandgap excitation for the GaN and InGaN epilayer samples discussed above. The strength of this feature decreased both with decreasing pump intensity and increasing detuning.

In further analogy with the InGaN epilayer, a broad bleaching is observed in the InGaN MQW barrier region (3.13 - 3.30 eV) for all excitation energies. The peak of the carrier distribution is observed at the 3.23 eV barrier energy. For above- and near-bandgap excitation in Fig. 8a and Fig. 8b, the blue edge of this carrier distribution rises faster (300 fs, 360 fs) than the red edge (540 fs, 560 fs) in the QWs. This is reminiscent of the carrier redistribution for above bandgap (3.35 eV) excitation in the InGaN epilayer (Fig. 4a).

Likewise, the blue edge of the MQW carrier distribution, centered at the 3-D barrier band edge (3.23 eV), is observed to decay much faster than the red edge (blue:10ps, red:>100ps). As in the InGaN epilayer (Fig. 4a), this initial fast decay of the blue edge corresponds to the SE-related fast decay in the spectrally-integrated TRDT. However, the carriers cool down to the barrier band edge more quickly (<1 ps) than they did for above bandgap excitation of the InGaN epilayer, resulting in a very broad (170 meV) carrier distribution extending from the GaN edge down into the QWs. This difference between epilayer and MQW barrier carrier relaxation arises because capture into the QWs removes carriers from the InGaN barrier much faster than recombination removes them from the InGaN epilayer.[20]

The role of SE-mediated carrier relaxation is most clearly seen by comparing the at-bandgap excitation TRDT data above ($300~\mu J/cm^2$) (Fig. 8b) and below (60 $\mu J/cm^2$) (Fig. 8d) threshold. In the first 1 ps, the larger, asymmetric carrier distribution for the above threshold data is obvious, indicating the greater carrier concentration in the barriers and the role of SE in effectively depleting the higher energy barrier states faster than the band edge barrier states. Although carrier capture is apparent, a large percentage of carriers remain in the barrier region while SE is operating. By contrast, the below threshold
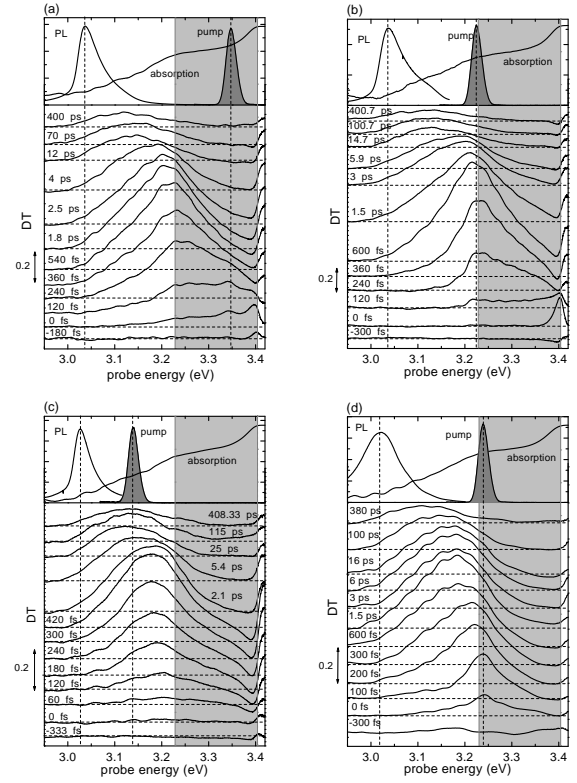

FIG. 8: Spectrally-resolved TRDT for above- (a), at- (b), and below-barrier (c) energy excitations at various delays for an excitation power density of 300 $\mu J/cm^2$. Pulsed absorption shows a clear absorption edge at ~ 3.23 eV, and the shaded regions indicate the states between the barrier and the GaN band edges. (d) shows the TRDT data for at-barrier excitation with a lower power density of 60 $\mu J/cm^2$.

TRDT data indicates a more symmetric carrier distribution whose relaxation rates are much less sensitive to carrier energy and whose peak drops below the barrier band energy in only 300 fs. By 1.5 ps, the below threshold carrier distribution is fully 50 meV below that of the above threshold case, and the barriers are virtually depopulated. It may be surmised that SE assists in the carrier capture process by quickly depopulating QW states which are refilled by captured barrier band edge carriers which in turn are refilled by higher energy carriers in the barriers. The normal cooling of the carrier distribution observed below threshold is altered above threshold by SE through the continued emptying of energetically accessible states near the barrier band edge. By 6 ps when SE is over, however, the distributions appear quite similar and exhibit the same relaxation behavior thereafter.

In addition to elucidating the action of SE and carrier redistribution, Fig. 8 reveals the mechanism of QW carrier capture. Due to their higher density of states, holes are expected to be captured from the 3-D barriers to the 2-D QW levels much faster than the electrons.[38] Pulse widths of 100 fs used here limit our observations to the electron capture. A significant number of carriers are ob-
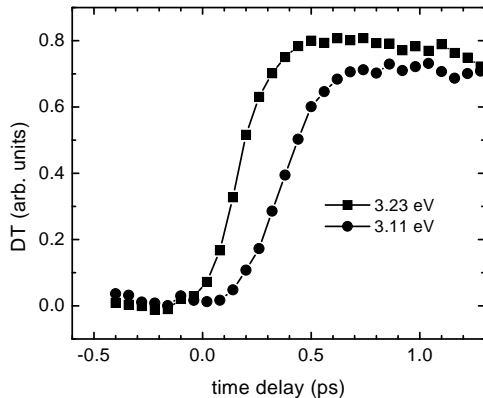
FIG. 9: Normalized DT at barrier (3.23 eV, squares) and the QW band edge(3.11 eV, circles) energies for the at-barrier energy excitation (300 μJ/cm^2). The rise of the DT at QW energy is slower than the rise of the signal at the barrier energy, indicating electron capture into the confined QW states.

served at and above the barriers after 240 fs for above- and at-barrier excitations, while carriers are just beginning to appear in the QWs (Fig. 8b). The carrier distribution at the barrier band edge (3.23 eV) peaks in ~ 0.5 ps, while the carrier distribution at the QWs (3.11 eV) reaches its maximum in ~ 0.8 ps (Fig. 9). This delay of 0.3 ps confirms that the carriers are reaching the barriers faster than they arrive at the QWs, an indication of the electron capture process. This result is consistent with previous measurements of electron capture time (340-510 fs) using degenerate TRDT spectroscopy.[20]

In addition, degenerate TRDT showed optimal emission efficiency and most efficient carrier capture occurred when the carrier injection was within ± 40 meV of the 3.23 eV barrier energy.[20] Similar to the cw-absorption measurements (Fig. 1), the pulsed absorption spectrum in Fig. 8 clearly shows an 80 meV-wide peak centered at 3.23 eV. This broad absorption suggests potential fluctuations in the barriers due to the compositional inhomogeneities. The spectrally-integrated DT data obtained here verifies that the most efficient carrier capture occurs for pump energies near the barrier energy.

Measurements by Satake et al.[11] also show a broad distribution of carriers around the barrier energy and SE-related decays faster than 5 ps in the spectrally-resolved DT. However, the QW capture rate could not be observed. Other studies on InGaN-based laser diode structures by Kawakami et al.[10,24] also observed the same fast carrier accumulation at the barriers and much slower SPE decay from the QWs. It is not clear if those samples, excited at power densities above the SE threshold, show the same initial fast decay feature in the spectrally-integrated DT signals as seen here. However, carrier capture to the lower energy localized QW states appears to occur in less than 1 ps, similar to our measurements. Surprisingly, a

sizable carrier population remains at barrier energies for at least 200 ps in their samples, which they claim is due to the capture of carriers in a high lying, nearly delocalized QW state. However, this feature bears some similarity to the long-lived excitonic relaxation in GaN interfacial traps observed in our InGaN TRDT data (FIG. 4). By contrast, the broad, quickly decaying distribution of carriers observed in our MQW sample is probably due to rapid carrier capture from the broad absorption at the barrier energy (Fig. 8).

For an excitation energy (3.14 eV) below the barriers, total carrier generation is smaller, and the peak carrier distribution appears at a slightly lower energy than the other two excitation energies (Fig. 8c). Unlike below-band edge (3.23 eV) excitation in the InGaN epilayer, the MQW carrier distribution is observed to peak 50 meV below the barrier edge. Nevertheless, both the InGaN and MQW carrier distributions reach their maximum in a very short time ($\sim$400 fs), and the rise times for both blue and red edges of the respective carrier distributions (Fig. 4b and Fig. 8c) are similar. This behavior contrasts with the above- and at- bandgap excitation for the MQW in which the blue side rises faster than the red side. As observed in Fig. 7, the fast decaying component of the spectrally-integrated DT for the below-barrier excitation is smaller than for the other two excitations, indicating a weaker carrier decay through SE. Accordingly, f is very small for the spectrally-integrated DT, and the blue edge decay of the TRDT signal in Fig. 8c is not noticeable.

The fast decaying component in the spectrally-integrated TRDT signal disappears as the carrier density falls below the SE threshold and emission goes from SE to SPE.[10,11,24] After SE ends (5 - 10 ps), the carriers at the QW band edge recombine only through SPE, and carriers at higher energies relax at a similar rate to replace those lost at the QW band edge. For all excitations this is observed as the redshift of the bleaching. The carrier distribution cools and redshifts to the QW band edge (~ 3.11 eV) after 400 ps. In addition to carrier recombination in the QWs, the redshift of the carrier distribution is also partly due to the reduced screening of the PZE field as carrier density decreases through SPE.[10] An exponential fit to the spectrally-resolved data at 3.11 eV gives a decay constant of 0.66±0.06 ns, consistent with the 0.69 ns value from previous degenerate TRDT measurements.[20] The slow decay constant from the spectrally-integrated TRDT is slightly smaller (0.54±0.07 ns), but agrees satisfactorily when the carrier redistribution through different channels is taken into account.

IV. CONCLUSIONS

In summary, non-degenerate TRDT spectroscopy is performed on a bulk GaN layer, an InGaN epilayer, and an InGaN MQW. All the samples were observed to have SE features for excitation densities above a pump threshold density of $\sim$100μJ/cm^2. Spectrally-integrated TRDT

data showed the effects of SE-mediated decay, which occurred in <10 ps for above band gap excitations. These fast decays are accompanied by carrier relaxation from higher to lower energy states which are emptied in turn by SE. After the total carrier density is reduced below threshold, SE disappeared and a slow relaxation through SPE is observed. For GaN, a spectrally narrow absorption of carriers decayed by SE at the band edge in 6 ps. A broader carrier distribution is observed for the InGaN sample which narrowed and decayed to the InGaN band edge through SE in <14 ps. Carrier recombination through spontaneous emission was observed with a time constant of approximately 1 ns.

Photo-excitation above, at, and below the barrier energy for the MQW sample showed more complex relaxation pathways in the QWs. Spectrally-integrated TRDT signals for above- and at-barrier bandgap energy excitations demonstrated SE as a fast decaying component in the first 10 ps. The strength and fast decay times of the SE feature were seen to vary as a function of excitation energy and density. For a given excitation density, the decay times varied inversely with the PLE magnitudes for the respective excitation energy. SE was observed to depopulate the higher energy barrier states faster than the lower energy barrier states through a process of cascaded refilling. Once SE ended, carrier capture and spontaneous emission from carrier recombination cools the carrier distribution into the wells and toward the lowest energy QW state. The wavelength non-degenerate TRDT data at QW and barrier energies provided sub-ps values for the electron capture time, and ∼660 ps for the recombination time. These values agree well with previous degenerate TRDT measurements on the same MQW sample.[20]

* Email address: everitt@aro.arl.army.mil

[1] S. Nakamura and G. Fasol, *The Blue Laser Diode*, Springer, Berlin 1997, and references therein.

[2] S. Nakamura, M. Senoh, N. Iwasa, and S. Nagahama, Jpn. J. Appl. Phys. **34**, L797 (1995).

[3] S. Nakamura, M. Senoh, S. Nagahama, N. Iwasa, T. Yamada, T. Matsushita, H. Kiyoku, Y. Sugimoto, T. Kozaki, H. Umemoto, M. Sano, and K. Chocko, Jpn. J. Appl. Phys., Part 2 **36**, L1568 (1997).

[4] J. C. Carrano, T. Li, P. A. Grudowski, C. J. Eiting, R. D. Dupuis, and J. C. Campbell, J. Appl. Phys. **83**, 6148 (1998).

[5] S. Chichibu, T. Sota, K. Wada, and S. Nakamura, J. Vac. Sci. Technol. B **16**, 2204 (1998).

[6] E. Berkowicz, D. Gershoni, and G. Bahir, E. Lakin, D. Shilo, E. Zolotoyabko, A. C. Abare, S. P. DenBaars, and L. A. Coldren, Phys. Rev. B **61**, 10994 (2000).

[7] S. F. Chichibu, A. C. Abare, M. P. Mack, M. S. Minsky, T. Deguchi, D. Cohen, P. Kozodoy, S. B. Fleischer, S. Keller, J. S. Speck, J. E. Bowers, E. Hu, U. K. Mishra, L. A. Coldren, S. P. DenBaars, K. Wada, T. Sota, and S. Nakamura, Mater. Sci. Eng. B **59**, 298 (1999).

[8] C. K. Choi, B. D. Little, Y. H. Kwon, J. B. Lam, J. J. Song, Y. C. Chang, S. Keller, U. K. Mishra, and S. P. DenBaars, Phys. Rev. B **63**, 195302 (2001).

[9] K. Omae, Y. Kawakami, Y. Narukawa, Y. Watanabe, T. Mukai, and S. Fujita, Phys. Stat. Sol. A 190, **93** (2002).

[10] Y. Kawakami, Y. Narukawa, K. Omae, S. Fujita, and S. Nakamura, Appl. Phys. Lett. **77**, 2151 (2000).

[11] A. Satake, Y. Masumoto, T. Miyajima, T. Asatsuma, and M. Ikeda, Phys. Rev. B **60**, 16660 (1999).

[12] R. W. Martin, P. G. Middleton, K. P. O'Donnell, and W. Van der Stricht, Appl. Phys. Lett. **74**, 263 (1999).

[13] P. Riblet, H. Hirayama, A. Kinoshita, A. Hirata, and T. Sugano, Appl. Phys. Lett. **75**, 2241 (1999).

[14] A. Satake, Y. Masumoto, T. Miyajima, T. Asatsuma, F. Nakamura, and M. Ikeda, Phys. Rev. B **57**, R2041 (1998).

[15] J. K. Shmagin, J. F. Muth, R. M. Kolbas, S. Krishnankutty, S. Keller, U. K. Mishra, and S. P. DenBaars, J. Appl. Phys. **81**, 2021 (1997).

[16] T. J. Schmidt, S. Bidnyk, Y. H. Cho, A. J. FIsher, J. J. Song, S. Keller, U. K. Mishra, and S. P. DenBaars, Appl. Phys. Lett. **73**, 3689 (1998).

[17] T. J. Schmidt, Y. H. Cho, G. H. Gainer, J. J. Song, S. Keller, U. K. Mishra, and S. P. DenBaars, Appl. Phys. Lett. **73**, 560 (1998).

[18] S. Bidnyk, T. J. Schmidt, Y. H. Cho, G. H. Gainer, J. J. Song, S. Keller, U. K. Mishra, and S. P. DenBaars, Appl. Phys. Lett. **72**, 1623 (1998).

[19] S. Keller, S. F.Chichibu, M. S. Minsky, E. Hu, U. K. Mishra, and S. P. DenBaars, J. Cryst. Growth **195**, 258 (1998).

[20] Ü. Özgür, M. J. Bergmann, H. C. Casey, Jr., H. O. Everitt, A. C. Abare, S. Keller, and S. P. DenBaars, Appl. Phys. Lett. **77**, 109 (2000).

[21] J. F. Muth, J. H. Lee, I. K. Shmagin, R. M. Kolbas, H. C. Casey, Jr., B. P. Keller, U. K. Mishra, and S. P. DenBaars, Appl. Phys. Lett. **71**, 2572 (1997).

[22] K. Omae, Y. Kawakami, S. Fujita, M. Yamada, Y. Narukawa, and T. Mukai, Phys. Rev. B **65**, 073308 (2002).

[23] C. K. Choi, Y. K. Kwon, J. S. Krasinski, G. H. Park, G. Setlur, J. J. Song, and Y. C. Chang, Phys. Rev. B **63**, 115315 (2001).

[24] Y. Kawakami, K. Omae, A. Kaneta, K. Okamoto, Y. Narukawa, T. Mukai, and S. Fujita, J. Phys.:Condens. Matter **13**, 6993 (2001).

[25] W. D. Herzog, G. E. Bunea, M. S. Ünlü, B. B. Goldberg, and R. J Molnar, Appl. Phys. Lett. **77**, 4145 (2000)

[26] J. C. Holst, L. Eckey, A. Hoffman, I. Broser, H. Amano, and I. Akasaki, MRS Int. J. Nitride Semicond. Res. **2**, 25

(1997).

[27] S. Jursenas, N. Kurilcik, G. Kurilcik, A. Zukauskas, P. Prysyawko, M. Leszcynski, T. Suski, P. Perlin, I. Grzegory and S. Porowski, Appl. Phys. Lett. **78**, 3776 (2001).

[28] C. K. Choi, J. B. Lam, G. H. Gainer, S. K. Shee, J. S. Krasinski, J. J. Song, and Y.-C. Chang, Phys. Rev. B **65**, 155206 (2002).

[29] This cooling is not observed in TRDT due to high absorption above the GaN band edge.

[30] C. Wetzel, T. Takeuchi, S. Yamaguchi, H. Katoh, H. Amano, and I. Akasaki, Appl. Phys. Lett. **73**, 1994 (1998)

[31] M. D. McCluskey, C. G. Van de Walle, C. P. Master, L. T. Romano, and N. M. Johnson, Appl. Phys. Lett. **72**, 2725 (1998).

[32] K. P. Korona, P. Prystawko, M. Leszczynski, P. Perlin, T. Suski, I. Grzegory, S. Porowski, and J. Kuhl, Mater. Sci. Eng. B **93**, 73 (2002).

[33] T. Takeuchi, C. Wetzel, S. Yamaguchi, H. Sakai, H. Amano, I. Akasaki, Y. Kaneko, S. Nakagawa, Y. Yamaoka, and N. Yamada, Appl. Phys. Lett. **73**, 1691 (1998).

[34] Y.-H. Cho, J. J. Song, S. Keller, M. S. Minsky, E. Hu, U. K. Mishra, and S. P. DenBaars, Appl. Phys. Lett. **73**, 1128 (1998).

[35] S. F. Chichibu, A. C. Abare, M. S. Minsky, S. Keller, S. B. Fleischer, J. E. Bowers, E. Hu, U. K. Mishra, L. A. Coldren, S. P. DenBaars, and T. Sota, Appl. Phys. Lett. **73**, 2006 (1998)

[36] It should be noted that part of the DT signal at the GaN band edge is excluded from the spectral integration to avoid obfuscation by the AC Stark effect.

[37] Note that a tiny SE feature remains even below the threshold due to pump and sample inhomogeneities.

[38] N. S. Mansour, K. W. Kim, and M. A. Littlejohn, J. Appl. Phys. **77**, 2824 (1995).